

SIMULATIONS OF POSITRON CAPTURE AT Ce^+BAF^*

A. Ushakov^{1†}, J. Benesch¹, J. Grames¹, S. Nagaitsev¹, N. Raut¹, R. Rimmer¹, Y. Roblin¹,
E. Voutier², S. Wang¹

¹Thomas Jefferson National Accelerator Facility, Newport News, USA

²Université Paris-Saclay, CNRS/IN2P3/IJCLab, Orsay, France

Abstract

We present a capture concept for the continuous wave (CW) polarized positron injector for the Continuous Electron Beam Accelerator Facility (CEBAF) at Jefferson Lab (Ce^+BAF). This two-step concept is based on (1) the generation of bremsstrahlung radiation by a longitudinally polarized electron beam (1 mA, 120 MeV, 90% polarization), passing through a tungsten target, and (2) the production of e^+e^- -pairs by these bremsstrahlung photons in the same target. To provide highly-polarized positron beams (>60% polarization) or high-current positron beams (>1 μA) with low polarization for nuclear physics experiments, the positron source requires a flexible capture system with an adjustable energy selection band. The results of beam dynamics simulations and calculations of the power deposited in the positron capture section are presented.

INTRODUCTION

The positron production and polarization transfer from a CW longitudinally polarized electron beam to positrons via bremsstrahlung radiation and e^+e^- -pair production in high-Z conversion target, referred as the PEPPo (Polarized Electrons for Polarized Positrons) technique [1], has been adopted to generate positrons at the Ce^+BAF [2]. The initial beam dynamics simulations have shown that the Ce^+BAF injector concept based on the PEPPo technique is capable of delivering the required positron currents within the acceptance limits of the CEBAF accelerator [3, 4]. Only a small fraction of the positrons generated in the tungsten target by the 120 MeV electron beam are captured. The positron yield, defined as the number of positrons within the CEBAF acceptance per primary electron, is in the range from $5 \cdot 10^{-5}$ to $1 \cdot 10^{-3}$, depending on the energy of positrons selected by the capture system from a wide energy spectrum at the target exit (shown in the next section). Therefore, a high current drive electron beam of 1 mA is required and most ($\geq 90\%$) of the 120 kW beam power is absorbed by the 4 mm thick tungsten target and in a few meters of the positron capture system downstream target. The target, capture magnets and cavity are currently being developed by the Ce^+BAF team. In this paper, we present the results of positron capture simulations and calculations of the power absorbed in the capture system components with realistic geometries and fields.

* This work is supported by the U.S. Department of Energy, Office of Science, Office of Nuclear Physics under contract DE-AC05-06OR23177; U.S. Department of Energy, Office of Science, U.S.-Japan Science and Technology Cooperation Program in High Energy Physics, DOE National Laboratory Program Announcement Number LAB 23-2858.

† ushakov@jlab.org

GEOMETRY AND FIELDS

The main components at the beginning of the positron injector (target, focusing solenoid and embedded in the solenoid cavity) were included in the simulations. The model of capture section also includes the shielding inside the focusing solenoid and absorbers in the area between the focusing solenoid and the cavity. The geometry used in the simulations is shown in Fig. 1.

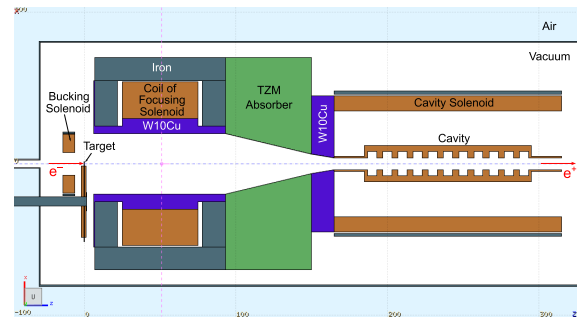


Figure 1: Geometry of target and e^+ capture section.

The concept of a rotated, water-cooled, 4 mm thick tungsten target was evaluated [5]. Calculations of target temperature, mechanical stress and radiation damage have shown that the target with an outer diameter of 38 cm rotated at a frequency of 2 Hz can be cooled (the peak temperature is 680°C) and the annual radiation damage is ~ 0.2 dpa. The work on the target design is continuing [6].

The field strength of the focusing solenoid and the length and inner radius of the shielded solenoid were optimized to maximize the current of 60 MeV positrons at the cavity exit. The 60 MeV was chosen because the figure of merit, defined as the product of the positron current and the square of its longitudinal polarization, is maximal at this energy and target thickness [7]. The optimal field distribution of the focusing and bucking solenoids is shown in Fig. 2. The focusing solenoid consists of a copper coil 50 cm long, 30 cm inner radius, 54 cm outer radius and 15 cm thick steel with an inner radius of 25 cm. The bucking solenoid compensates for the field in the rotated target. Both solenoids use the same 15 mm square insulated conductor with an 11 mm hole for cooling water. The focusing solenoid coil consists of 33 turns per layer, 16 layers, and each layer has a separate water circuit. At the coil current density of 446 A/cm², the 1.03 T field on the beam axis is 50 cm from the target and 18 bar, ~ 500 cm³/s water flow is sufficient for cooling. A low-field cavity solenoid (50 mT) is used in the calculations presented below. The magnetic field profile on beam axis is shown in Fig. 3.

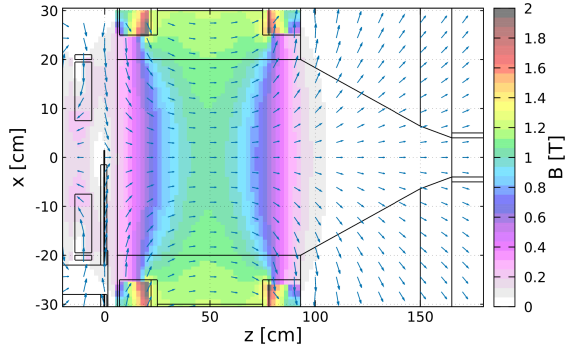


Figure 2: Magnetic field distribution of focusing and bucking solenoids.

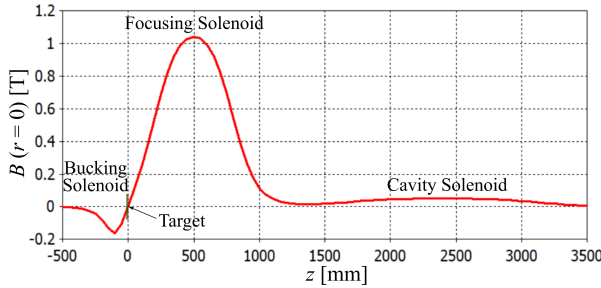


Figure 3: B-field profile on beam axis.

SIMULATIONS OF POSITRON CAPTURE AND POWER ABSORPTION

FLUKA [8,9] was used to track particles and calculate the energy deposited by beams in the target and positron capture system. Figure 4 shows the distribution of the number of positrons per cubic centimeter and per primary electron (positron yield density) and demonstrates the focusing of positrons by the capture system based on 1.03 T solenoid.

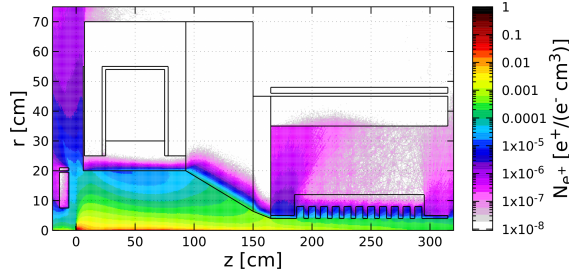


Figure 4: Distribution of positron yield density.

The distribution of power density deposited by beams is shown in Fig. 5. The power absorbed in target and components of capture system is listed in Table 1. The highest fraction of the beam power (55 kW) is deposited in the TZM absorber (99.4% Mo, 0.5% Ti, 0.1% Zr) downstream of the focusing solenoid. Significant fractions of the power are also deposited in the target (18.3 kW) and in the W10Cu (90%W-10%Cu) absorbers shielding the focusing solenoid (18.7 kW) and in front of the capture cavity (12.6 kW). 8.5 kW is deposited by beams in the cavity. Work on the shielding design, cooling system and thermal assessment will be continued

and alternative shielding materials will be considered. The target and capture components absorb approximately 96 percent of the 120 kW primary beam power. Table 2 shows how the remaining power of 4.8 kW is distributed among electrons, positrons, and photons at the cavity exit, as well as their intensity (yield) and average energy. The initial energy spectra of e^- , e^+ and γ at the target exit and at the cavity entrance and exit are shown in Fig. 6. The capture system with a 1.03 T focusing solenoid helps to filter electrons and positrons and to retain particles with an energy of ~ 60 MeV.

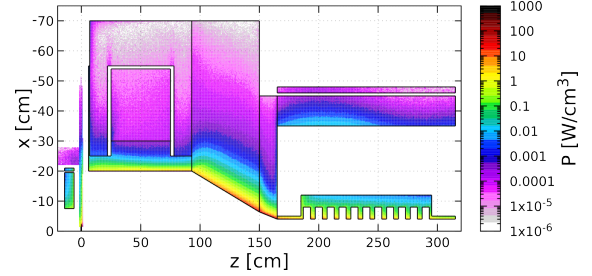


Figure 5: Distribution of power deposited by beams.

Table 1: Power absorbed in target and components of positron capture system.

Power of beams and absorbed power	Power [kW]
Primary e^- beam	120.00
<i>Absorbed beam power:</i>	
Bucking solenoid	0.74
Target	18.32
Coil of focusing solenoid	0.02
Iron of focusing solenoid	0.07
W10Cu shielding of focusing solenoid	18.68
TZM absorber	54.96
W10Cu absorber	12.61
Cavity	8.50
Cavity solenoid	0.62
Vacuum chamber and pipe	0.60
Total absorbed beam power	115.12
Power of γ , e^- and e^+ at cavity exit	4.76

Table 2: Yield, average energy and power of photons, electrons and positrons at cavity exit.

Yield/Energy/Power	γ	e^-	e^+
Yield [$N_{\gamma, e^-, e^+} / N_{e^-}$]	0.152	0.040	0.008
Average energy [MeV]	13.06	50.54	33.78
Beam power [kW]	1.99	2.03	0.27

The General Particle Tracer (GPT) code [10] was used to calculate the beam polarization and to correctly track beams in the RF cavity field. Such calculations are not possible in FLUKA. The initial beam and fields were imported into

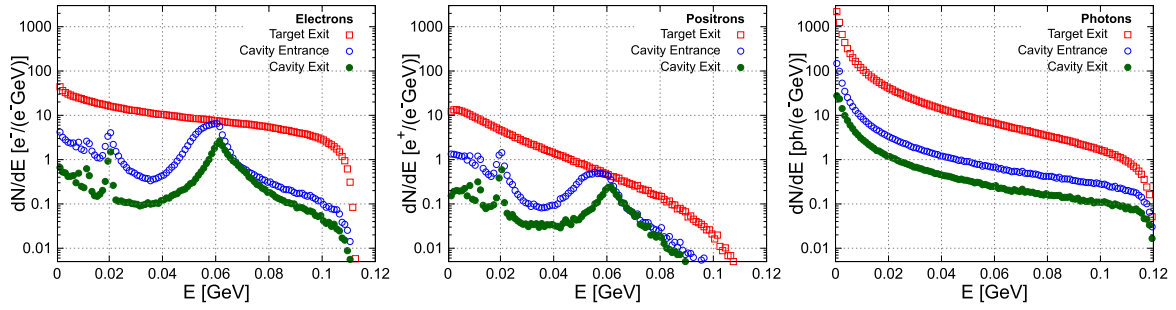


Figure 6: Energy spectra of electrons, positrons and photons at target exit, cavity entrance and exit (calculated in FLUKA).

GPT from other simulation codes. The 6D distribution of positrons at the target exit and their polarization were calculated in Geant4 [11, 12]. CST Studio Suite [13] was used to calculate the magnetic field of solenoids. The work on design of the CW normal conducting standing wave cavity has begun recently [14]. ACE3P (Advanced Computational Electro-magnetics 3D Parallel) [15] was used to design the cavity and generate 3D field maps for GPT simulations.

The results of beam tracking presented below are based on the 1497 MHz 11-cell cavity with an iris radius of 4 cm and a peak gradient of 3 MV/m. The longitudinal (time-energy) phase space at the cavity exit is shown in Fig. 7. The 1.03 T solenoid, optimized for focusing 60 MeV positrons, also captures positrons at lower energies. The multiple peaks in the energy spectrum are consistent with a simplified theoretical model of positron capture by a short strong solenoid followed by a long weak solenoid, usually called a Quarter-Wave Transformer (QWT) [4].

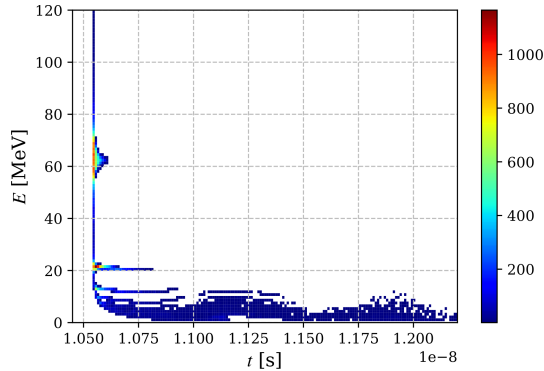


Figure 7: Longitudinal phase space of positrons at cavity exit (calculated in GPT).

The transverse phase space of positrons with energies corresponding to three main peaks of the energy spectrum (62.5 MeV, 21 MeV and 12.8 MeV) and 2% energy spread is shown in Fig. 8. Table 3 lists the current, normalized emittance, bunch length and polarization of positrons from these energy bands. The 62.5 MeV positrons have significantly higher polarization (71.9%), shorter bunch length (4.5 mm) and higher normalized emittance (11.4 mm-rad). The 50 nA goal current for the high-polarization option of the Ce⁺BAF injector and the 609 nA current at the exit of the capture cavity leave room for the development of emittance

filters. The experiments with a degraded electron beam, which are planned for this summer at CEBAF, will allow a better determination of the Ce⁺BAF acceptance [16, 17].

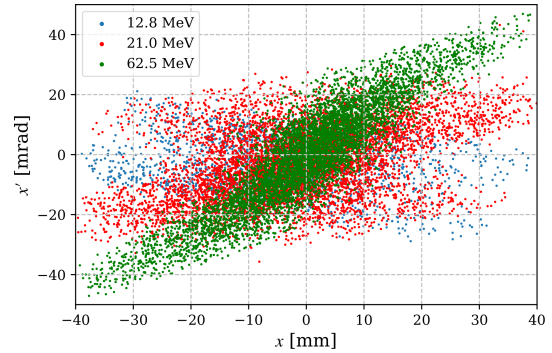


Figure 8: xx' phase space of positrons with 2% energy spread and three different energies at cavity exit.

Table 3: Parameters for positrons with different energies.

Energy [MeV]	62.5	21.0	12.8
Energy spread [%]	2		
Current [nA]	609	678	156
Normalized emittance [mm-rad]	11.4	6.3	3.8
Bunch length σ_z [mm]	4.5	11.3	8.4
Polarization [%]	71.9	26.5	15.9

OUTLOOK

The development of the Ce⁺BAF capture magnets and cavities and the simulation of the positron capture is a tightly coupled iterative process. First beam tracking simulations in realistic geometries and fields show promising results. The concept of the Ce⁺BAF injector, based on a rotated water-cooled tungsten target, a focusing solenoid with ≈ 1 T peak field on the beam axis, and a CW standing wave capture cavity, is capable of providing the required current of positrons with more than 60% polarization. The design of injector components, thermal and mechanical stress analysis, radiation damage and induced radioactivity calculations, and design of required shielding will be continued.

REFERENCES

- [1] D. Abbott *et al.*, “Production of highly polarized positrons using polarized electrons at MeV energies”, *Phys. Rev. Lett.*, vol. 116, p. 214801, 2016. doi:10.1103/PhysRevLett.116.214801
- [2] J. Grames *et al.*, “Positron beams at Ce⁺BAF”, in *Proc. 14th Int. Particle Accelerator Conf. (IPAC’23)*, Venice, Italy, May 2023. paper MOPL152, pp. 896–899. doi:10.18429/JACoW-IPAC2023-MOPL152
- [3] S. Habet *et al.*, “Concept of a polarized positron source for CEBAF”, in *Proc. 13th Int. Particle Accelerator Conf. (IPAC’22)*, Bangkok, Thailand, June 2023. paper MOPOTK012, pp. 457–459. doi:10.18429/JACoW-IPAC2022-MOPOTK012
- [4] S. Habet, “Concept of a polarized positron source for CEBAF”, Ph.D. thesis, Paris-Saclay University, France, Dec. 2023.
- [5] A. Ushakov *et al.*, “Evaluation of a high-power target design for positron production at CEBAF”, in *Proc. 14th Int. Particle Accelerator Conf. (IPAC’23)*, Venice, Italy, May 2023. paper WEPM120, pp. 3842–899. doi:10.18429/JACoW-IPAC2023-3844
- [6] K. Mahler *et al.*, “Computational fluid dynamics design of a very high-power rotating positron target”, presented at IPAC’24, Nashville, TN, USA, May 2024, paper THPS46, this conference.
- [7] S. Habet, A. Ushakov, and E. Voutier, “Characterization and optimization of polarized and unpolarized positron production”, Tech. Rep. PEPPo TN-23-01, JLAB-ACC-23-3794, Feb. 2023. doi:10.48550/arXiv.2401.04484
- [8] C. Ahdida *et al.*, “New Capabilities of the FLUKA Multi-Purpose Code”, *Frontiers in Physics*, vol. 9, paper 788253, 2022. doi:10.3389/fphy.2021.788253
- [9] G. Battistoni *et al.*, “Overview of the FLUKA code”, *Ann. Nucl. Energy*, vol. 82, pp. 10–18, 2015. doi:10.3389/fphy.2021.788253
- [10] General Particle Tracer (GPT) code, <https://www.pulsar.n1/gpt/>
- [11] J. Allison *et al.*, “Recent Developments in Geant4”, *Nucl. Instrum. Meth. A*, vol. 835, pp. 0186–225, 2016. doi:10.1016/j.nima.2016.06.125
- [12] S. Agostinelli *et al.*, “Geant4 – A Simulation Toolkit”, *Nucl. Instrum. Meth. A*, vol. 506, pp. 250–303, 2003. doi:10.1016/S0168-9002(03)01368-8
- [13] CST Studio Suite, <https://www.3ds.com/products/simulia/cst-studio-suite>
- [14] S. Wang *et al.*, “Capture cavities for the CW polarized positron source Ce+BAF”, presented at IPAC’24, Nashville, TN, USA, May 2024, paper MOPC51, this conference.
- [15] ACE3P (Advanced Computational Electro-magnetics 3D Parallel), <https://confluence.slac.stanford.edu/display/AdvComp/ACE3P++Advanced+Computational+Electromagnetic+Simulation+Suite>
- [16] A. Sy *et al.*, “Towards large phase space beams at the CEBAF injector”, presented at IPAC’24, Nashville, TN, USA, May 2024, paper MOPC53, this conference.
- [17] V. Lizárraga-Rubio *et al.*, “Computational simulations and beamline optimizations for an electron beam degrader at CEBAF”, presented at IPAC’24, Nashville, TN, USA, May 2024, paper MOPC62, this conference.